Journal of ELECTRONIC MATERIALS, Vol. 37, No. 6, 2008
DOI: 10.1007/s11664-008-0396-5

Regular Issue Paper

The Shear Strength and Fracture Behavior of Sn-Ag-*x*Sb Solder Joints with Au/Ni-P/Cu UBM

HWA-TENG LEE,[1,2] SHUEN-YUAN HU,[1] TING-FU HONG,[1] and YIN-FA CHEN[1]

1.—Department of Mechanical Engineering, National Cheng-Kung University, Tainan, Taiwan, ROC. 2.—e-mail: htlee@mail.ncku.edu.tw

This study investigates the effects of Sb addition on the shear strength and fracture behavior of Sn-Ag-based solders with Au/Ni-P/Cu underbump metallization (UBM) substrates. Sn-3Ag-*x*Sb ternary alloy solder joints were prepared by adding 0 wt.% to 10 wt.% Sb to a Sn-3.5Ag alloy and joining them with Au/Ni-P/Cu UBM substrates. The solder joints were isothermally stored at 150°C for up to 625 h to study their microstructure and interfacial reaction with the UBM. Single-lap shear tests were conducted to evaluate the mechanical properties, thermal resistance, and failure behavior. The results show that UBM effectively suppressed intermetallic compound (IMC) formation and growth during isothermal storage. The Sb addition helped to refine the Ag_3Sn compounds, further improving the shear strength and thermal resistance of the solders. The fracture behavior evolved from solder mode toward the mixed mode and finally to the IMC mode with increasing added Sb and isothermal storage time. However, SnSb compounds were found in the solder with 10 wt.% Sb; they may cause mechanical degradation of the solder after long-term isothermal storage.

Key words: Lead-free solders, intermetallic compounds, underbump metallization, failure mode, thermal storage

INTRODUCTION

Tin-lead (Sn-Pb) solders are widely used in the electronics industry due to a combination of many technical advantages, such as excellent solderability, workability, thermal and electrical conductivity, mechanical reliability, and low cost. Concerns about using Pb in the electronics industry have been raised for many years, mainly stemming from occupational exposure, Pb waste from the manufacturing process, and the disposal of electronic assemblies. Pb use is being limited by stricter legislation.[1] These factors have stimulated extensive research and development efforts to invent novel lead-free solder alloys to substitute for Sn-Pb solders in electronic applications.

In the past, copper (Cu) was extensively used in the substrate metallization and the underbump metallization (UBM) for chip ball-grid arrays (BGA) packaging applications. However, the rapid formation and thickening of Cu-Sn intermetallic compounds (IMC) at the tin-rich solder/Cu interface during reflowing process attracted serious concerns about the reliability of these solders.[2–6] Hence, the Cu pad does not make contact with the solder balls directly in current BGAs. Gold (Au) and nickel (Ni) layers are normally deposited on top of the Cu pad to suppress the Cu_3Sn and Cu_6Sn_5 IMC layer coarsening effect, with Ni acting as a diffusion barrier and Au being utilized to prevent Ni surfaces from oxidizing to promote interfacial solderability.[7–9] Phosphorus (P) is usually used with Ni because hypophosphite plating baths are generally used for reducing Ni ions.[7]

UBMs are normally made using sputter, evaporation, and electroplated coating technologies. In recent years, there has been increasing interest in producing UBMs using electroless plating methods[3,9–12] due to their favorable advantages of low

(Received May 31, 2007; accepted January 18, 2008; published online February 22, 2008)

manufacturing cost, uniform thickness and low residual intrinsic stresses, and selective depositions. Many studies[3,6,9,13,14] have also investigated the interfacial reactions between electroless Ni-based UBMs and Sn-based solder alloys, and Ni_3Sn_4 has been identified as the main IMC layer that forms after soldering and reflowing.

Recently, studies[15,16] have shown that adding antimony (Sb) can refine the Ag_3Sn precipitate and hence improve the mechanical properties and thermal resistance of the Sn-Ag-based solder with Cu substrates. The present study investigates how Sb additions influence the microstructure evolution and the shear strength of Sn-Ag-based solders after being stored at an elevated temperature for various periods of time with electrolessly plated Au/Ni-P/Cu UBM.

EXPERIMENTAL PROCEDURE

Solder Preparation

Various fractions of high-purity Sb were smelted with Sn-3.5Ag alloy at 600°C in a crucible protected with nitrogen to fabricate Sn-3Ag-*x*Sb (x = 2 wt.%, 4 wt.%, and 10 wt.%) solders. The target and actual composition of the solders produced in the study, which was identified by the inductively coupled plasma-atomic emission spectrometry (ICP-AES) technique, can be seen in Table I. In order to produce solder balls with a consistent size for preparing the solder joint with Cu plates, the bulk solder was first rolled into a 0.09-mm-thick sheet and then punched into tiny circular discs of 6 mm diameter. After immersing these circular discs in an oil at 300°C, the melted solder transformed into a ball-like shape due to the high surface tension. When cooled at room temperature, the solder balls (Fig. 1) were found to have a diameter of roughly 1.7 mm. The solder balls were cleaned using acetone before being used in the subsequent process for microstructure characterization and single-lap shear strength assessments.

Single-Lap Tests and Microstructure Characterization

Single-lap tests were used to simulate actual solder joints in use and to evaluate the shear strength of the synthesized solders. The specimens for single-lap tests were prepared by joining a solder ball between the Au/Ni-P/Cu substrates. High-purity (>99.95%) copper was used as a substrate material. It was cut into plates of 50 mm × 10 mm × 1 mm. The Ni-P deposition was carried out by electroless plating on the Cu substrate at 82°C for 30 min in a solution with a pH value of 4.0 to 4.6. A thin Au film was immediately sputter-coated on top of the Ni-P deposition to prevent oxidation of the Ni surface. To join the solder ball with the two UBM substrates, the solder ball was placed between the UBM substrates, which were separated by two spacers to maintain a fixed height. The specimens were then clamped and pre-heated at 190°C to 200°C for 15 min, and then reflowed at 270°C to 280°C for 3–4 min in an electronic oven. The final specimen is schematically shown in Fig. 2, where the solder joint has an hourglass shape with a fixed height of 0.8 mm. The specimens were also isothermally stored at 150°C for up to 625 h to investigate their microstructure and thermal resistance. The single-lap tests were conducted at room temperature using a Shimadzu AG-I universal testing machine with a constant cross-head velocity of 0.5 mm/min. A field-emission scanning electron microscope (FE-SEM, Philips XL 40FEG) was used for microstructural and fractural analyses. Energy dispersive X-ray spectroscopy (EDX) was performed in the FE-SEM to analyze the chemical composition of the structures.

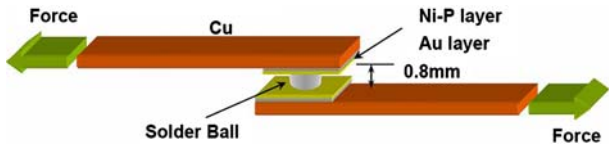

Fig. 1. Illustration of single-lap shear test specimen.

Table I. The Target and Actual Solder Compositions Used in the Study

Solder	Chemical Composition (wt.%)		
	Sn	Ag	Sb
Sn-3.5Ag	Bal.	3.5	–
Sn-3Ag-2Sb	Bal.	2.9	1.7
Sn-3Ag-4Sb	Bal.	3.1	3.9
Sn-3Ag-10Sb	Bal.	3.1	10.1

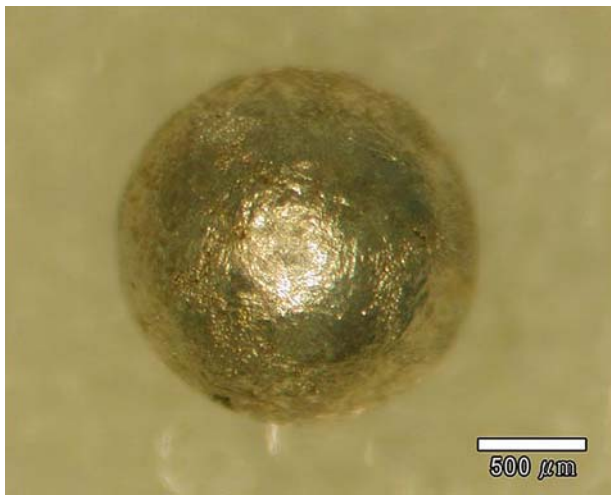

Fig. 2. Morphology of the solder ball produced in the study.

RESULTS AND DISCUSSION

Microstructure Characterization

The solder joints prepared with Au/Ni-P/Cu UBM had a fixed height and diameter of around 0.8 mm and 1.8 mm, respectively. Figure 3 shows the optical microscopy images of as-soldered joints and their counterparts after isothermal storage at 150°C for 625 h. The images reveal that Au/Ni-P/Cu UBM effectively helped to suppress IMC formation and growth; the thickness of IMCs was in the submicron range in the as-soldered samples and between 4 μm and 6 μm after heat storage. Among the as-soldered samples, Sn-3.5Ag had the largest amount of Ag_3Sn compounds. Because of the nonequilibrium solidification process, the β-Sn matrix regions were surrounded by a large number of Ag_3Sn particles. Furthermore, an increase in Sb addition resulted in a decrease of Ag_3Sn formation in the solder. No distinct Ag_3Sn was found in the solder with 10% Sb content, but $Ag_3(Sn, Sb)$ and SnSb[15,16] were observed instead.

To identify the existence of Sb in the solder, the solders were characterized using SEM with EDX. Sb existed inside the solder in two forms (Fig. 4): dissolved in the β-Sn matrix or precipitated as Sb-rich phases. Therefore, the addition of Sb not only assists to suppress the formation of Ag_3Sn but may also help to provide solute and precipitate mechanisms to strengthen the Sn-Ag-Sb solder.

Comparing the microstructures before and after isothermal storage at 150°C for 625 h in Fig. 3, it can be seen that the addition of Sb can effectively ease the Ag_3Sn coarsening effect of thermal storage. However, in the Sn-3Ag-10Sb samples, the size of $Ag_3(Sn, Sb)$ and the cubic-shaped SnSb precipitates increased significantly with an increase of isothermal storage period.

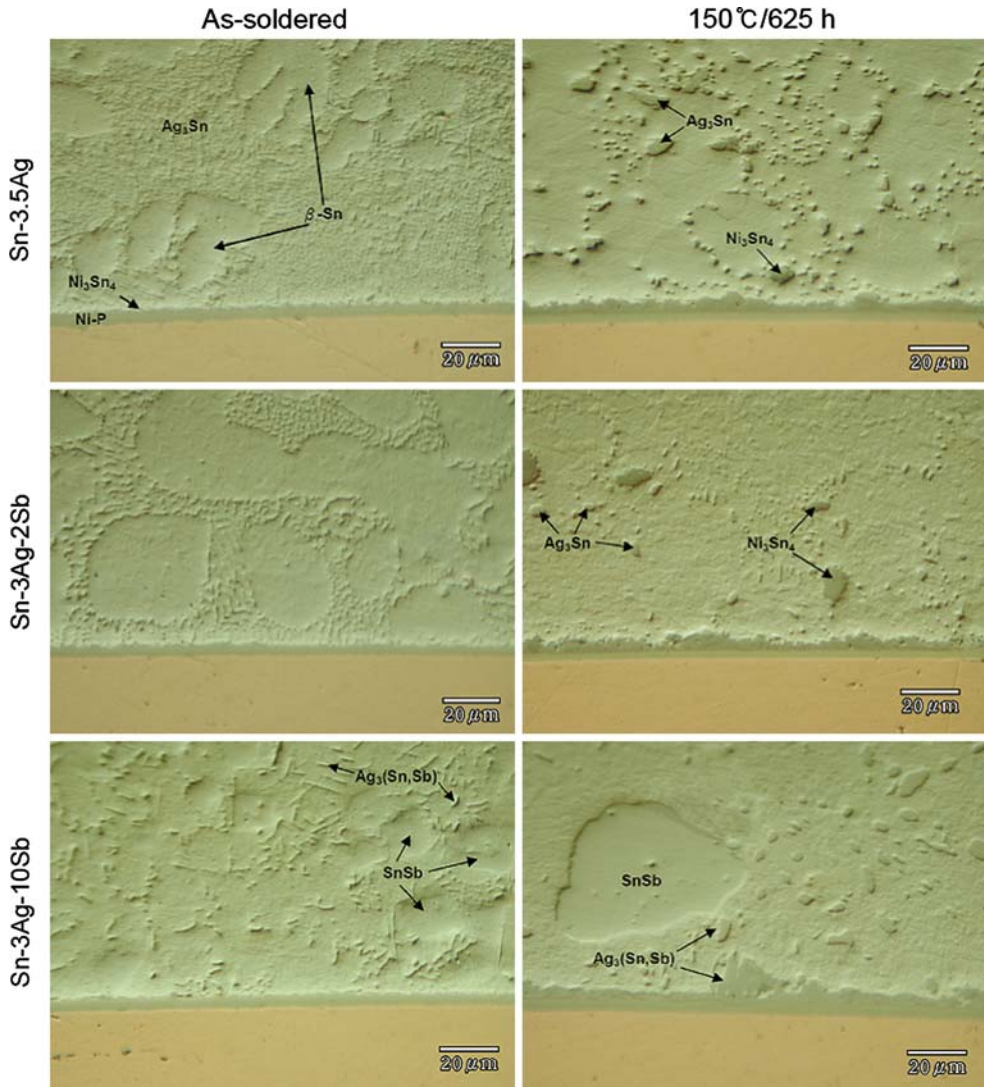

Fig. 3. Optical microscope images of as-soldered joints and their counterparts after isothermal storage at 150°C for 625 h.

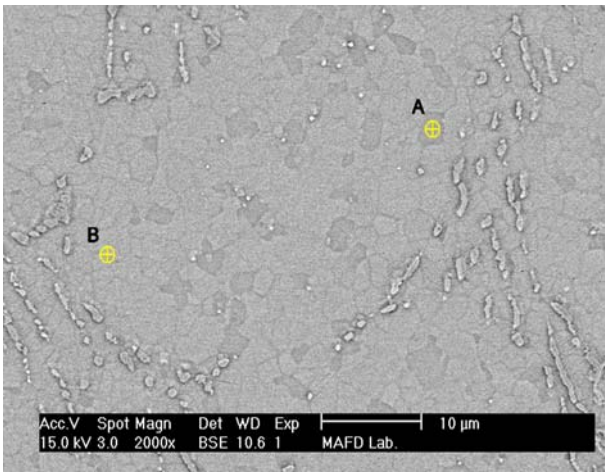

	Element	Wt%	At%
A	Ag L	1.4	1.6
	Sn L	69.9	70.3
	Sb L	28.7	28.1
	Total	100.0	100.0
B	Ag L	1.0	1.1
	Sn L	97.2	97.1
	Sb L	1.8	1.8
	Total	100.0	100.0

Fig. 4. SEM back-scattered electron (BSE) image with EDX analyses of as-soldered Sn-3Ag-4Sb.

Shear Strength Measurements

Figure 5 shows the shear strength evolution of the Sn-3.5Ag and Sn-3Ag-*x*Sb solder joints with Au/Ni-P/Cu UBM after storage at 150°C for various periods of time. It can be seen that the shear strength of the solder joints increases with increasing Sb addition, but decreases with increasing isothermal storing time. According to the research in Ref. 17, the solder may be strengthened by the solid-solution effect in the low Sb content range. By adding increasing amounts of Sb, the formation of SnSb compounds in the solder may further increase the joint strength. However, after the heat storage processes, because of the precipitates coarsening and IMC thickening effects, the shear strength of the solders decreases with isothermal storage time (Fig. 5). Nevertheless, the decreasing slope of the profile eventually reaches a plateau stage with time, except that of the solder with 10% Sb. This may be caused by the SnSb compounds, whose size was dramatically increased in the solder after isothermal storage, as can be seen in Fig. 3.

Fractography of Solder Joints

The fracture surfaces of the solder joints were examined after single-lap shear tests in order to investigate their fracture mechanism. Three fracture modes were found in the samples: in the solder, mixed solder/IMC, and in the IMC. The fracture mechanisms of these three modes were illustrated by Lee et al.[16] In the solder mode, cracks initiate on the surface of the solder joint and propagate within the solder; in the mixed solder/IMC mode, cracks initiate on the surface of the solder joint, propagate across the solder, and make contact with the IMC layer of the solder adjoining to the UBM substrate; and in the IMC mode, the cracks initiate near the IMC layer and propagate all along the interface.

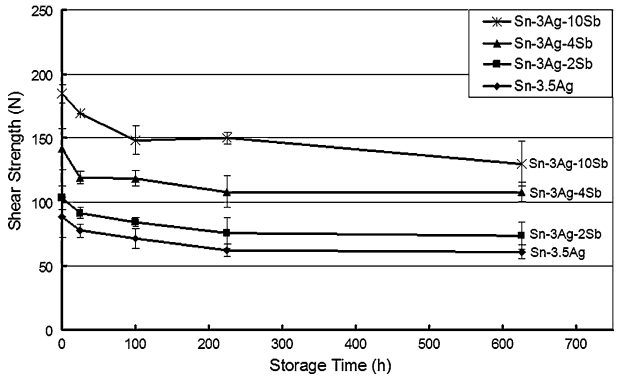

Fig. 5. The shear strength evolution of solder joints after isothermal storage for various periods of time.

In the as-soldered samples, it was observed that most of the joints fractured in the solder, except for the sample with 10% Sb content, in which the joints were fractured mostly in the IMC. This indicates that in most cases the solder/UBM interface is stronger than the solder. However, because of the alloy strengthening effects, the solder strength increases as the amount of added Sb increases. As a result, the strength of the solder is higher than that of the IMC. Thus, the fracture type gradually changes from the solder mode to the mixed mode and eventually to the IMC mode.

As mentioned before, the microstructure of the solder changes with the isothermal storage time, which directly affects its fracture mechanism. The stereo macroscopy images in Fig. 6 reveal the fracture morphology of the solder joints with 4% Sb addition after isothermal storage for 0 h, 225 h, and 625 h, respectively. The images clearly indicate that the fracture mode of the solder was changed with increasing thermal storage time. The as-soldered sample fractured entirely in the solder (Fig. 6a), whereas its counterpart after thermal storage for 225 h fractured partially in the solder and IMC (Fig. 6b), and the one after thermal storage for 625 h fractured mostly in the IMC (Fig. 6c). Since UBM can effectively suppress IMC formation, the degradation of shear strength coupled with the transformation of the fracture mode with the isothermal storage time are mainly due to the changes of the solder microstructure and properties.

The fractured surface of the heat-stored samples with various Sb additions can be seen in Figs. 7–9. Figure 7 shows the fracture surface morphology of

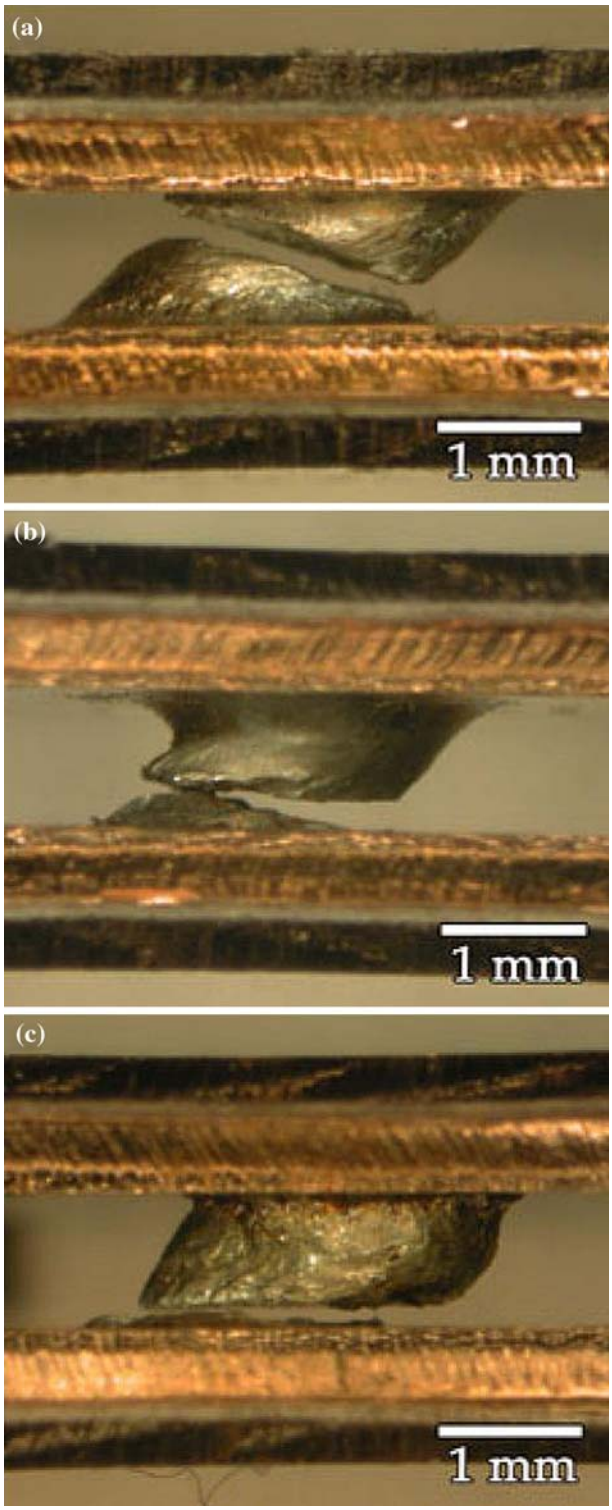

Fig. 6. Fracture morphology of Sn-3Ag-4Sb solder joints with UBM after isothermal storage for various periods of time: (a) as-soldered, (b) 150°C for 225 h, and (c) 150°C for 625 h.

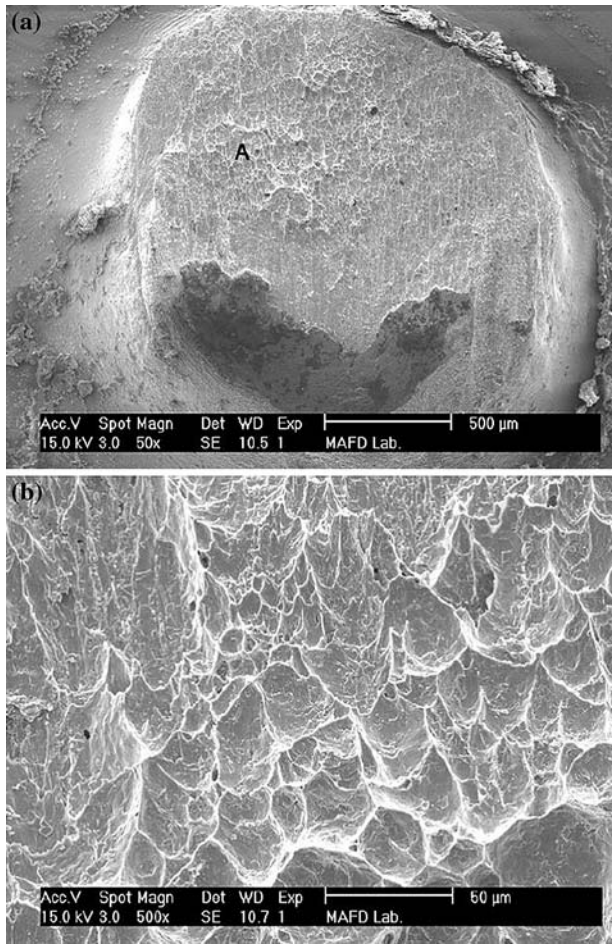

Fig. 7. The fracture surface images of Sn-3.5Ag after isothermal storage at 150°C for 625 h: (a) whole fractured solder joint and (b) magnified image of area A.

the Sn-3.5Ag solder after isothermal storage for 625 h. Figure 7a reveals that the sample was fractured mostly in the solder. The enlarged image of area A (Fig. 7b) shows that the solder was fractured via a plastic ductile deformation, in which lots of dimples with smooth walls and bottoms were formed on the fracture surfaces. Figure 8 shows the fracture surface morphology of the Sn-3Ag-4Sb solder joint after isothermal storage for 625 h. In Fig. 8a, it can be seen that the surface on the top-right side has a ductile fracture whereas the part on the bottom-left side shows a brittle fracture. Figure 8b shows the magnified image of area A in Fig. 8a, where a few Ag_3Sn precipitates can be observed on the dimple walls. In addition, compared with the smooth solder matrix dimple bottoms in Fig. 6b, Ni_3Sn_4 fragments from IMC were picked up at the dimple bottoms in Fig. 8b, which shows an evident discrepancy between these two samples. Figure 9 shows the fracture surface morphology of the Sn-3Ag-10Sb solder joint that was isothermally stored for 625 h. In this figure, a typical IMC fracture mode, in which the solder joint was subjected to a brittle fracture deformation, is illustrated. Figure 9b shows a magnified image of area A in Fig. 9a, where three distinct fracture surfaces can be found, i.e., the residue of the solder matrix (intergranular

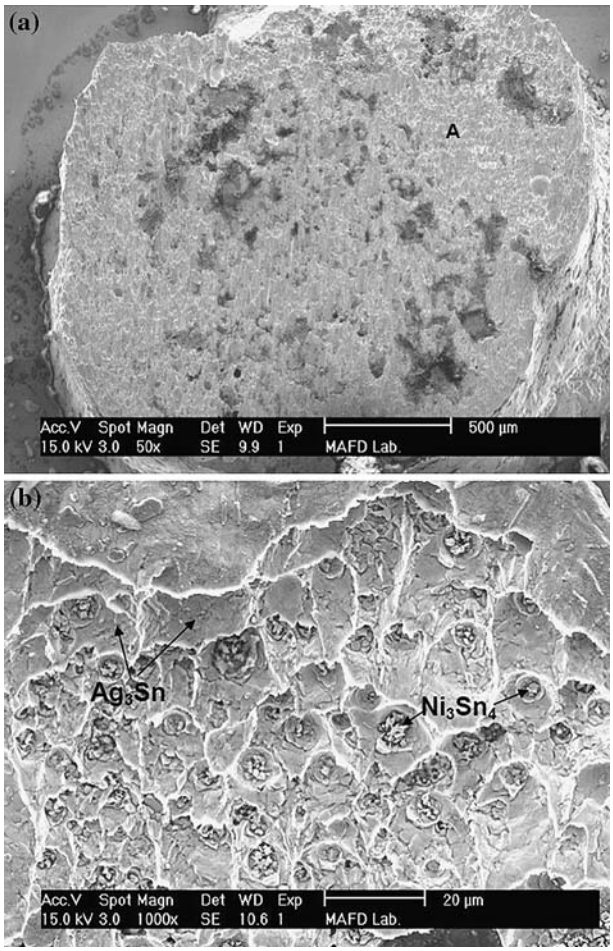

Fig. 8. The fracture surface images of Sn-3Ag-4Sb after isothermal storage at 150°C for 625 h: (a) whole fractured solder joint and (b) magnified image of area A.

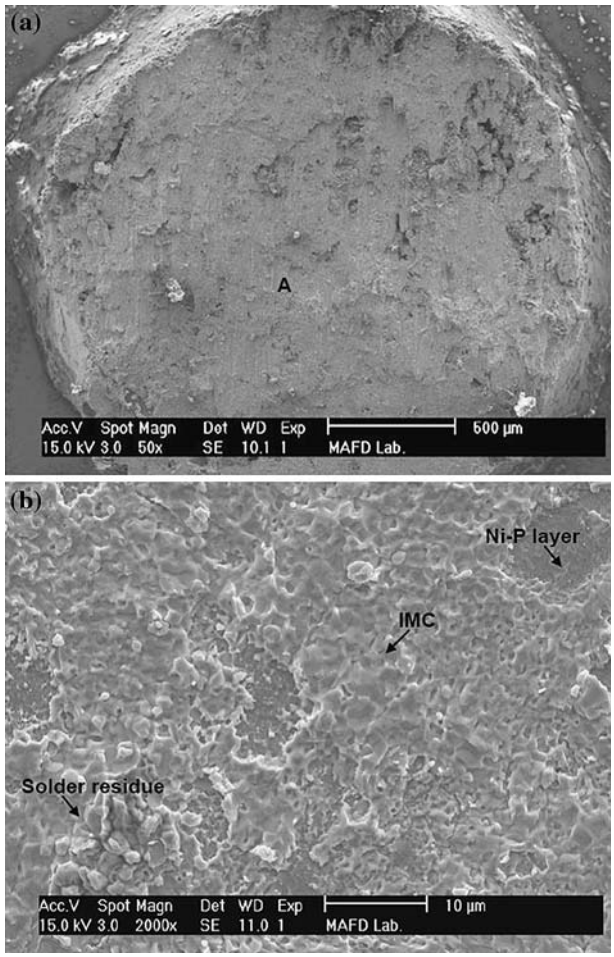

Fig. 9. The fracture surface images of Sn-3Ag-10Sb after isothermal storage at 150°C for 625 h: (a) whole fractured solder joint and (b) magnified image of area A.

fracture), the IMC layer (transgranular fracture), and the Ni-P layer.

Figure 10a–c schematically illustrates the cross-section of the localized area of solder joints fractured in the solder mode (Fig. 7b), the mixed solder/IMC mode (Fig. 8b), and the IMC mode (Fig. 9b), respectively. In the solder mode fracture (Fig. 10a), because the crack entirely occurs in the solder, the fracture surfaces are composed exclusively of solder residues (Fig. 7b). In contrast, in the mixed solder/IMC mode fracture, the crack propagates across the solder/IMC interfaces (Fig. 10b); therefore, both solder residues and Ni_3Sn_4 fragments (IMC) can be found in Fig. 8b, with the Ni_3Sn_4 at the bottom of the dimples. With a large amount of Sb, the fracture transits to the IMC mode; the crack yields in the IMC layer but sometimes it can reach the solder/IMC or IMC/Ni-P interface in the IMC mode fracture (Fig. 10c). All three layers can be observed on the fracture surfaces (Fig. 9b).

The transition of solder joint fracture modes can be explained by the change of strength and ductility in the solder.[16] The strength and brittleness of the

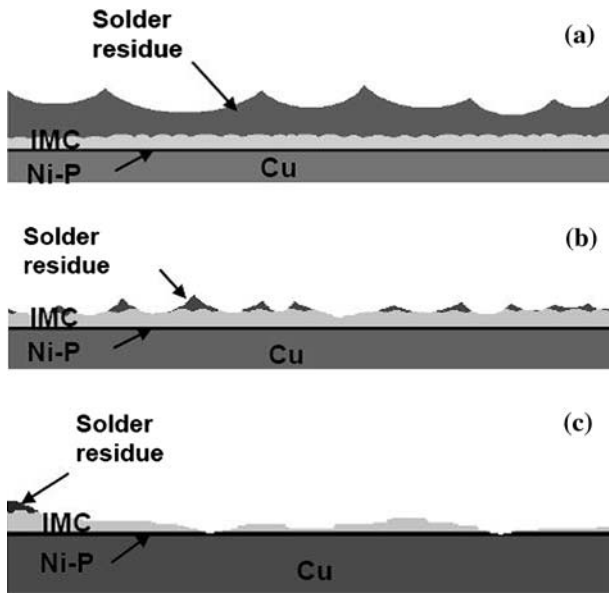

Fig. 10. Schematic illustration of the fractured solder joints in three different modes: (a) solder mode, (b) mixed solder/IMC mode, and (c) IMC mode joint.

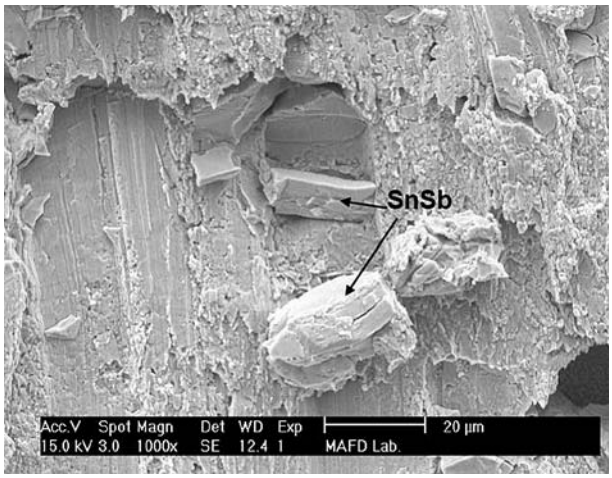

Fig. 11. An image of fractured SnSb compounds.

solder increase with increasing Sb content. As a result, the IMC/UBM layer may become the weakest part of the solder joint and yield plastic deformation, consequently initiating cracks in the IMC/UBM. The fracture interface changed from the interface of the solder/IMC to the interface of the IMC/UBM when the Sb content increased from 4% to 10%.

The coarsened SnSb compound in the heat-stored Sn-3Ag-10Sb sample is shown in Fig. 11, revealing a brittle fracture feature. These coarsened SnSb particles may provide a path for both intergranular and transgranular fractures, and thus weaken the solder mechanical properties. Further investigation on the properties of SnSb is essential to find its formation mechanism and to determine how it affects the fracture mechanisms of the Sn-Ag-Sb solders.

CONCLUSION

The microstructure and shear strength evolution of Sn-3.5Ag and Sn-3Ag-xSb solders with Au/Ni-P/Cu UBM before and after isothermal storage at 150°C for various periods of time were investigated in this study. The following conclusions can be drawn from the present results:

(1) Au/Ni-P/Cu UBMs can effectively suppress IMC formation and growth with Sn-3.5Ag and Sn-3Ag-xSb solders. The as-soldered IMCs have a submicron size thickness and only grow to 4 μm to 6 μm after isothermal storage at 150°C for up to 625 h.

(2) The addition of Sb not only results in a decrease of Ag_3Sn formation in the solder but can also effectively ease the Ag_3Sn coarsening effect during isothermal storage. Ag_3Sn nearly disappeared in the solder with 10% Sb content, with Ag_3(Sn, Sb) and SnSb compounds formed in the sample instead.

(3) Because of the alloy strengthening effects, the strength of the solder increases as the amount of added Sb increases. The fracture mode changes from the ductile solder mode to the brittle IMC mode. The coarsened SnSb particles may cause a degradation of the solder mechanical properties.

REFERENCES

1. The European Parliament and the Council of the European Union (Official Journal of the European Union, 2003), 37/24-38.
2. H.-T. Lee, M.-H. Chen, H.-M. Jao, and T.-L. Liao, *Mater. Sci. Eng. A* 358, 134 (2003).
3. J.W. Jang, P.G. Kim, K.N. Tu, D.R. Frear, and P. Thompson, *J. Appl. Phys.* 85, 8456 (1999).
4. C.Y. Liu, C. Chen, A.K. Mal, and K.N. Tu, *J. Appl. Phys.* 85, 3882 (1999).
5. K.N. Tu and K. Zeng, *Mater. Sci. Eng. R* 34, 1 (2001).
6. T. Laurila, V. Vuorinen, and J.K. Kivilahti, *Mater. Sci. Eng. R* 49, 1 (2005).
7. K. Zeng, V. Vuorinen, and J.K. Kivilahti, *IEEE Trans. Electron. Pack. Manuf.* 25, 162 (2002).
8. B.-L. Young, J.-G. Duh, and G.-Y. Jang, *J. Electron. Mater.* 32, 1463 (2003).
9. A. Kumar, M. He, and Z. Chen, *Surf. Coat. Technol.* 198, 283 (2005).
10. J. Kloeser, P. Coskina, R. Aschenbrenner, and H. Reichl, *Microelectron. Reliab.* 42, 391 (2002).
11. M.O. Alam, Y.C. Chan, and K.C. Hung, *Microelectron. Reliab.* 42, 1065 (2002).
12. M.O. Alam, Y.C. Chan, and K.C. Hung, *J. Electron. Mater.* 31, 1117 (2002).
13. J.W. Jang, D.R. Frear, T.Y. Lee, and K.N. Tu, *J. Appl. Phys.* 88, 6359 (2000).
14. K. Zeng, V. Vuorinen, and J.K. Kivilahti, *IEEE Trans. Electron. Pack. Manuf.* 25, 162 (2002).
15. H.-T. Lee, M.-H. Chen, H.-M. Jao, and C.-J. Hsu, *J. Electron. Mater.* 33, 1048 (2004).
16. H.-T. Lee, H.-S. Lin, C.-S. Lee, and P.-W. Chen, *Mater. Sci. Eng. A* 407, 36 (2005).
17. S.-Y. Hu (Master thesis, National Cheng-Kung University, 2003).